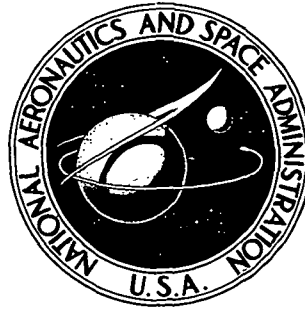


N72-32072

NASA TECHNICAL NOTE



NASA TN D-6967

NASA TN D-6967

CASE FILE
COPY



DESIGN AND COLD-AIR INVESTIGATION
OF A TURBINE FOR A SMALL
LOW-COST TURBOFAN ENGINE

by Milton G. Kofskey and William J. Nusbaum

*Lewis Research Center
Cleveland, Ohio 44135*

1. Report No. NASA TN D-6967	2. Government Accession No.	3. Recipient's Catalog No.	
4. Title and Subtitle DESIGN AND COLD-AIR INVESTIGATION OF A TURBINE FOR A SMALL LOW-COST TURBOFAN ENGINE		5. Report Date September 1972	
		6. Performing Organization Code	
7. Author(s) Milton G. Kofskey and William J. Nusbaum		8. Performing Organization Report No. E-6850	
		10. Work Unit No. 112-27	
9. Performing Organization Name and Address Lewis Research Center National Aeronautics and Space Administration Cleveland, Ohio 44135		11. Contract or Grant No.	
		13. Type of Report and Period Covered Technical Note	
12. Sponsoring Agency Name and Address National Aeronautics and Space Administration Washington, D.C. 20546		14. Sponsoring Agency Code	
		15. Supplementary Notes	
16. Abstract A 20.32-cm (8.00-in.) mean diameter two-stage turbine was investigated over a range of speeds from 0 to 110 percent of equivalent design speed and over a range of pressure ratios from 1.79 to 5.14. Presented are design information and turbine performance for first-stage and two-stage operation. Results are presented in terms of equivalent specific work, torque, mass flow, rotor exit flow angle, and efficiency.			
17. Key Words (Suggested by Author(s)) Axial flow turbine Efficiency Multistage turbine Performance tests Gas turbine		18. Distribution Statement Unclassified - unlimited	
19. Security Classif. (of this report) Unclassified	20. Security Classif. (of this page) Unclassified	21. No. of Pages 32	22. Price* \$3.00

* For sale by the National Technical Information Service, Springfield, Virginia 22151

DESIGN AND COLD-AIR INVESTIGATION OF A TURBINE
FOR A SMALL LOW-COST TURBOFAN ENGINE
by Milton G. Kofskey and William J. Nusbaum
Lewis Research Center

SUMMARY

An experimental investigation of a two-stage, 20.32-centimeter (8.00-in.) mean-diameter turbine was made to determine the performance level over a range of speeds and pressure ratios. The turbine was designed to drive the compressor and fan of a low-cost turbofan engine suitable for light aircraft application. Included in the report are design information and first-stage and two-stage performance results with cold air as the working fluid. Tests were made at speeds from 0 to 110 percent of equivalent design speed and pressure ratios from 1.79 to 5.14.

The results of the investigation indicated that, for two-stage operation, static and total efficiencies were 0.82 and 0.93, respectively. These values are significantly higher than the 0.780 and 0.880 assumed in the design. It should be pointed out that these higher efficiencies would not necessarily be expected to be obtained in actual engine operation. Losses due to nonuniform turbine-inlet conditions, increased interstage leakage, and increased tip clearance could result in efficiencies closer to the design values. The equivalent mass flow was about 0.8 percent larger than design at equivalent design speed and pressure ratio with two-stage operation. At this design point operation, first- and second-stage total efficiencies were 0.93 and 0.91 or six and four points higher than design, respectively. As a result, the stage work split was indicated to be 58 and 42 compared with the 57 to 43 split selected for the design.

First-stage performance indicated static and total efficiencies of 0.80 and 0.93, respectively. These values were five and six points higher than design, respectively. The equivalent mass flow at design point operation was about 0.8 percent larger than design. The measured stator throat area was found to be about 1 percent lower than design.

INTRODUCTION

Gas turbine engines are widely used in current large aircraft. This type of engine is also attractive as a replacement for the piston engine in single- and twin-engine light planes. A significant advantage of the gas turbine engine is its small size and weight per unit thrust as compared with the piston engine. One major problem in their use, however, is the high cost of the engine. Studies are being made at Lewis for achieving substantial cost reductions on the gas turbine engine (ref. 1). In order to achieve lower cost, the approach has been to use a very simply designed engine that would operate at moderate temperature levels and pressure ratio. By doing this, there would be a reduction in rotor blade speed, stress levels, and the number of stages from those used in present-day engines. Use of moderate temperatures would facilitate the use of low-cost fabrication techniques as well as low-cost materials.

Along these lines, design studies (ref. 1) have been made for a fan-jet engine to operate at cruise conditions of Mach 0.65 at an altitude of 7620 meters (25 000 ft). The engine has a cruise turbine-inlet temperature of 977.78 K (1760⁰ R) with an engine pressure ratio of 6 and a bypass ratio of 2.5. The mass-flow rate was 2.994 kilograms per second (6.6 lb/sec). The design mean rotor-blade speed is moderate at 297.9 meters per second (977.38 ft/sec). The design specific work for the two-stage turbine, selected for the engine was also conservative at values of 152.77 and 115.25 joules per gram (65.63 and 49.51 Btu/lb) for the first and second stage, respectively.

The turbine blading, having a mean diameter of 20.32 centimeters (8.00 in.) was designed and fabricated. A cold-air investigation of the turbine was then made to determine overall and stage performance. Turbine-inlet conditions were approximately constant at a temperature of 300 K (540⁰ R) and a pressure of 13.79 newtons per square centimeter (20 psia) for one-stage and 12.41 newtons per square centimeters (18.0 psia) for two-stage operations. The turbine was operated over a range of speeds from 0 to 110 percent of design and over a range of pressure ratio from 1.79 to 5.14.

This report presents design information and turbine performance for first-stage and two-stage operation. Test results are presented in terms of equivalent specific work, torque, mass flow, rotor-exit flow angle, and efficiency. A radial survey of rotor-exit flow angle is also presented for both first-stage and two-stage operations.

SYMBOLS

A area, cm²; in.²

D_p pressure-surface diffusion parameter, blade inlet relative velocity minus minimum blade surface relative velocity divided by blade inlet relative velocity

D_s	suction-surface diffusion parameter, maximum blade surface relative velocity minus blade outlet relative velocity divided by maximum blade surface relative velocity
D_{tot}	sum of suction- and pressure-surface diffusion parameter, $D_p + D_s$
g	dimensional constant, SI = 1.0; 32.174 ft/sec ²
Δh	specific work, J/g; Btu/lb
J	mechanical equivalent of heat, 778.2 ft-lb/Btu
N	turbine speed, rpm
p	pressure, N/cm ² abs; psia
R	gas constant, J/(kg)(K); ft-lb/(lb)(°R)
R_x	reaction, blade outlet velocity minus blade inlet velocity divided by blade outlet velocity
r	radius, m; ft
T	absolute temperature, K; °R
U	blade velocity, m/sec; ft/sec
V	absolute gas velocity, m/sec; ft/sec
V_j	ideal jet speed corresponding to total- to static-pressure ratio across turbine, m/sec; ft/sec
W	relative gas velocity, m/sec; ft/sec
w	mass flow, kg/sec; lb/sec
α	absolute gas flow angle measured from axial direction, deg
γ	ratio of specific heats
δ	ratio of inlet total pressure to U.S. standard sea-level pressure, p_1'/p^*
ϵ	function of γ used in relative parameters to those using air inlet conditions at U.S. standard sea-level conditions, $(0.740/\gamma)[(\gamma + 1)/2]^\gamma/(\gamma - 1)$
η_s	static efficiency (based on inlet total- to exit-static pressure ratio)
η_t	total efficiency (based on inlet total- to exit-total pressure ratio)
θ_{cr}	squared ratio of critical velocity at turbine inlet to critical velocity at U.S. standard sea-level air, $(V_{cr}/V_{cr}^*)^2$
λ	work-speed parameter, $U_m^2/gJ \Delta h$
ν	blade-jet speed ratio, U_m/V_j

τ torque, N-m; ft-lb

ω turbine speed, rad/sec

Subscripts:

cr condition corresponding to Mach number of unity

eq equivalent

m mean radius

u tangential component

w wall

1 station at turbine inlet (fig. 3)

2 station at first-stage stator exit (fig. 3)

3 station at first-stage rotor exit (fig. 3)

4 station at second-stage stator exit (fig. 3)

5 station at second-stage rotor exit (fig. 3)

Superscripts:

' absolute total state

* U.S. standard sea-level conditions (temperature equal to 288.15 K (518.67° R), pressure equal to 10.13 N/cm² (14.70 psia))

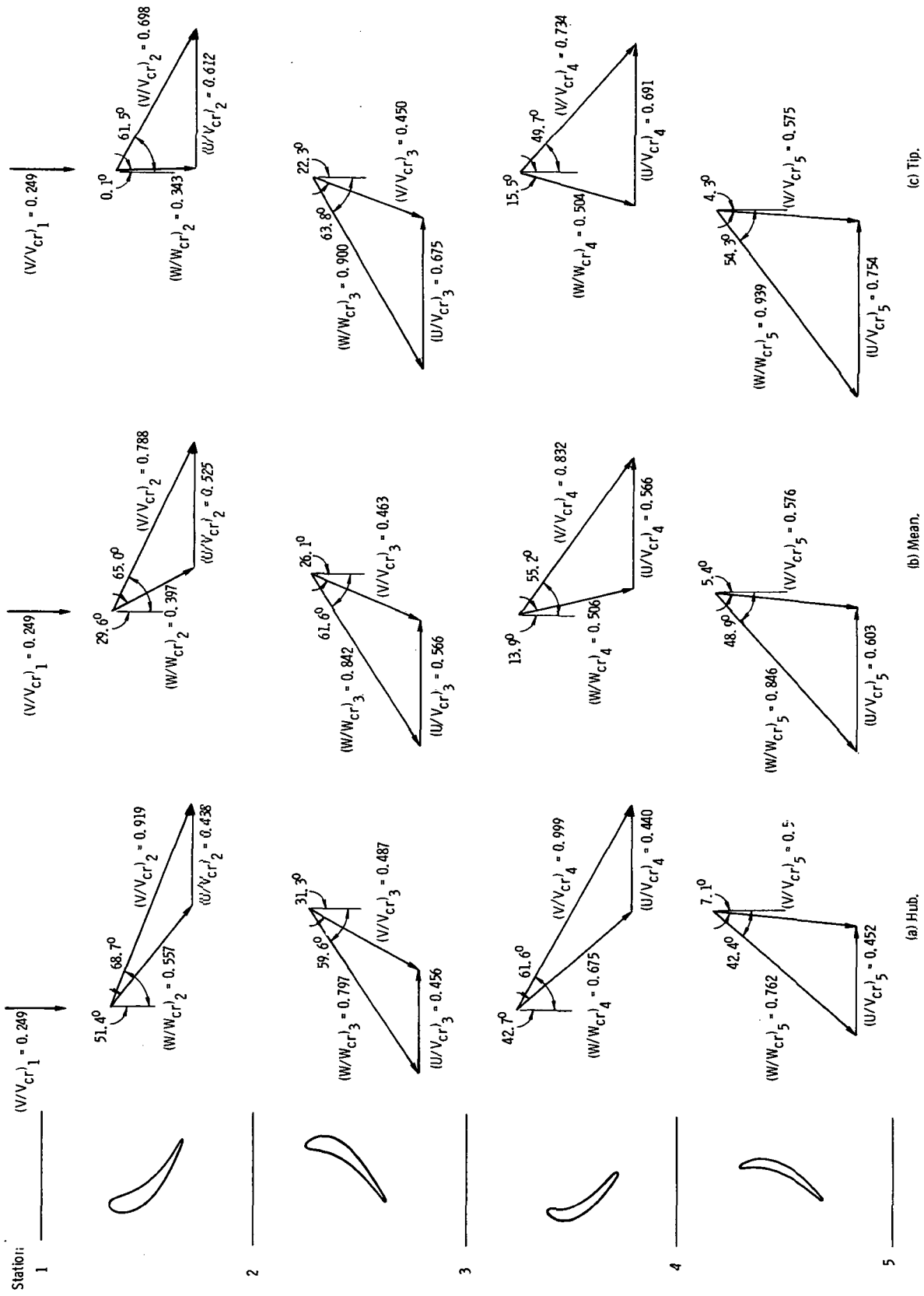
TURBINE DESIGN

Design Requirements

The design requirements for the 20.32-centimeter (8.0-in.) mean diameter two-stage turbine are given in table I. An overall work-speed parameter λ of 0.331 indicates a conservative design, which should be conducive to good aerodynamic efficiency. A turbine-inlet temperature of 977.78 K (1760° R) and a rotor-blade speed (mean section) of 297.91 meters per second (977.38 ft/sec) should not create any serious stress problems.

Velocity Diagrams

The free-stream velocity diagrams were computed to meet the design requirements and are based on the following assumptions:



(c) Tip.

(b) Mean.

(a) Hub.

Figure 1. - Design free-stream velocity diagrams.

- (1) A 57 to 43 percent work split between the first and second stages, giving respective values of work-speed parameters of 0.582 and 0.771
- (2) Respective losses in total pressure through the first- and second-stage stators of 4.0 and 5.0 percent of stage-inlet pressure
- (3) First-stage and two-stage total efficiency values of 0.870 and 0.880, respectively (These values of efficiency are based on material presented in ref. 2.)
- (4) Free vortex flow.

Design second-stage total and static efficiencies of 0.871 and 0.669, respectively, were calculated from these assumptions.

The free-stream velocity diagrams and station nomenclature are shown in figure 1. The amount of turning and the magnitude of velocities throughout the turbine indicate a conservative design. The turning at the mean diameter is 91.2° and 62.8° for the first- and second-stage rotors, respectively. All free-stream velocities are subsonic, with near sonic conditions existing at the exit of both stators at the hub. There is an increase in relative velocity through both rotors, indicating some positive reaction that increases from hub to tip. Values of reaction are presented in table II along with other aerodynamic parameters.

Stator Blades

The stator blade chord was determined from the axial dimension of the space allocated to the turbine by the engine design. The selection of blade number was based on the results of an optimum solidity study reported in reference 3. There are 35 and 43 blades in the first and second stages, respectively, with mean section blade chords of 2.616 and 2.182 centimeter (1.030 and 0.859 in.). Values of solidity at the mean sections are 1.43 and 1.47. The first-stage stator blade row has a constant blade height of 3.363 centimeters (1.324 in.); the second-stage stator blade height increases from 3.945 centimeters (1.553 in.) at the inlet to 4.483 centimeters (1.765 in.) at the exit. Both first- and second-stage blade rows have a constant mean diameter of 20.32 centimeters (8.0 in.). The stator-blade profile and stator-flow passages are shown in figures 2 and 3. The blade coordinates at hub, mean, and tip sections of both stators are shown in table III(a).

The stator-blade surface velocities were calculated by the computer program described in reference 4. The velocities that were obtained at the hub, mean, and tip sections are shown in figure 4 where the critical-velocity ratio is shown as a function of fractional surface length. In this computer program blade-surface velocities are calculated for only that part of the blade surface forming the guided channel. Accordingly, the curves in the figure do not extend over the entire length of the blade surface but, nevertheless, give a good indication of the velocity levels through the blade rows.

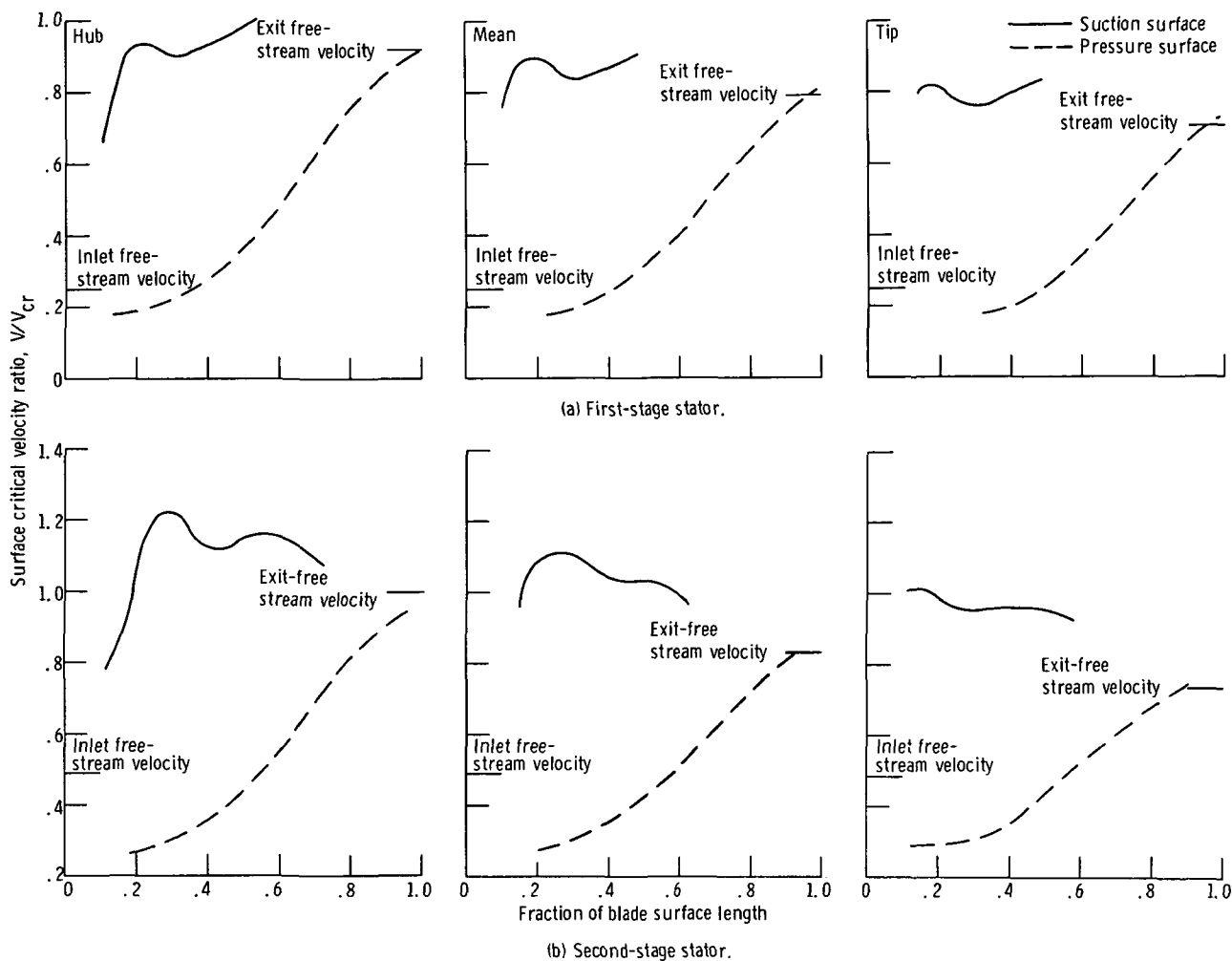


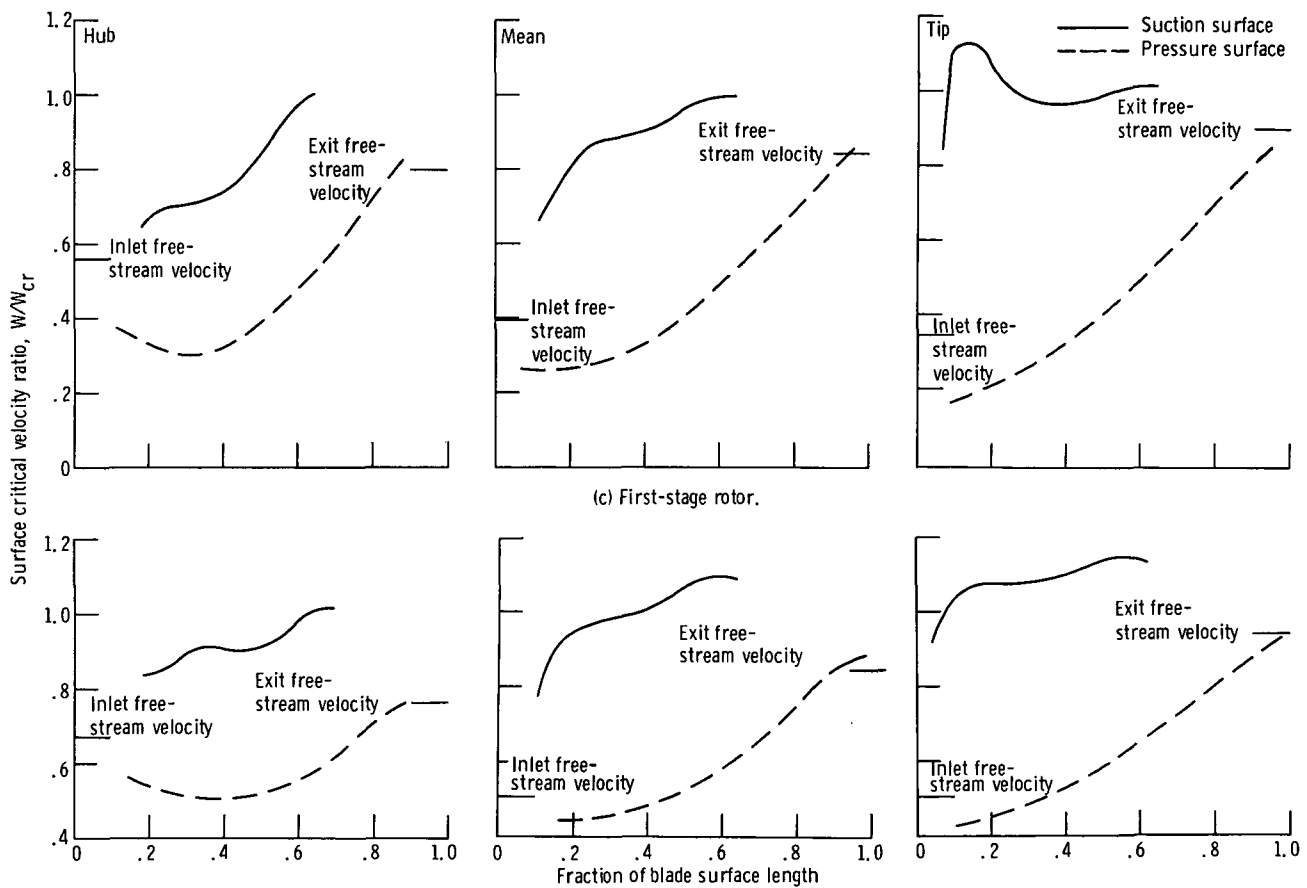
Figure 4. - Design surface velocity distributions at hub, mean, and tip sections.

The first-stage stator (fig. 4(a)) shows a rapidly accelerating flow on the suction surface in the region near the leading edge to a velocity level near that at the exit. This results in a suction-surface diffusion value of only 0.131 at the mean section. There is a deceleration of the flow on the pressure surface near the leading edge resulting in a pressure-surface diffusion value of 0.309.

The second-stage stator surface velocities show similar patterns, with mean section suction and pressure-surface diffusion values of 0.250 and 0.428, respectively. The low values of suction-surface diffusion for the two stators are considered favorable for high stator efficiency. The diffusion values for the pressure surfaces are larger but should not penalize turbine performance. Reference 5 concludes that turbine performance is not penalized by increased stator-blade loading (or increased pressure-surface diffusion) provided zero diffusion is maintained on the suction surface. Design values of diffusion, solidity, reaction, aspect ratio, etc., for all blade rows are given in table II.

Rotor Blades

The procedure used in the design of the stator blades was also used for the rotor blade design. There are 42 and 44 rotor blades in the first and second stages, respectively, giving values of solidity at the mean section of 1.71 and 1.66. The rotor-blade profiles and flow passages are shown in figures 2 and 3. The blade coordinates at the hub, mean, and tip sections of both rotors are given in table III(b). The inner and outer walls of the flow passage diverge equally at both blade rows (fig. 3), giving average blade heights of 3.658 and 4.801 centimeters (1.44 and 1.89 in.). The contour of the outer wall at the inlet to the first-stage rotor is designed to reduce the amount of leakage over the tips of the blades. This is done by a sharp corner just upstream of the leading edge. The tip clearance for the first-stage rotor is 0.030 centimeter (0.012 in.). The 0.038-centimeter (0.015-in.) tip clearance for the second-stage rotor blades is provided by a recess in the outer wall, thereby reducing leakage flow. These values of tip clearance are 0.8 percent of the respective annulus heights. In order to minimize leakage between



(d) Second stage rotor.

Figure 4. - Concluded.

stages, a labyrinth-shaft seal was machined on the second-stage stator. The seal is located on a 10.85-centimeter (4.27-in.) diameter with a clearance of 0.025 centimeter (0.010 in.) between seal and rotor hub. There are regions of constant flow area just upstream and downstream of the blading in order to facilitate accurate measurements of flow conditions.

The rotor-blade surface velocities at hub, mean, and tip sections are shown in figures 4(c) and (d). The difference in level between the suction- and pressure-surface velocities increases from hub to tip for both rotors. There is, also, a marked decrease in wetted area per unit blade height from hub to tip. The tip region of both rotors is, thus, more heavily loaded than the hub. Values of suction surface diffusion vary from 0.15 to 0.25. There is some deceleration of the flow on the pressure surface near the leading edge. However, the blade-surface velocities indicate a conservative design with no large values of diffusion on either the suction or pressure surfaces. Values of diffusion and other pertinent design parameters are summarized in table II. The two rotor assemblies are shown in figure 5. The blade twist is quite apparent in this figure.

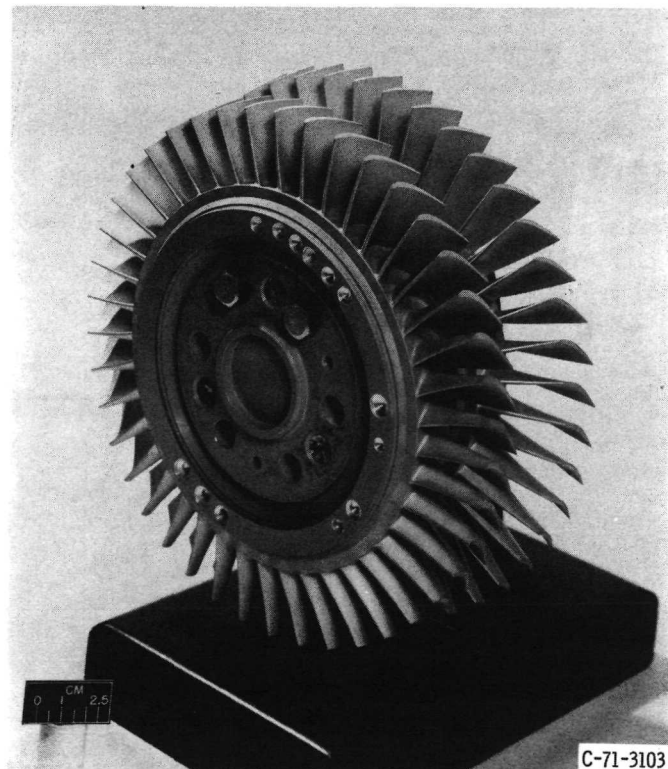


Figure 5. - Turbine rotors.

APPARATUS, INSTRUMENTATION, AND PROCEDURE

Apparatus

The apparatus consisted of the turbine, described in the preceding section, a cradled dynamometer to absorb the power output of the turbine while controlling the speed, and an inlet and exhaust piping system with flow controls. The arrangement of the apparatus is shown schematically in figure 6(a). High-pressure dry air was supplied from the laboratory air system. It passed through a filter, a weight flow measuring station consisting of a calibrated flat-plate orifice, a remotely controlled pressure-regulating valve, an inlet plenum, and into the turbine. After passing through the turbine, the air was exhausted through a system of piping and a remotely operated valve into the laboratory exhaust system.

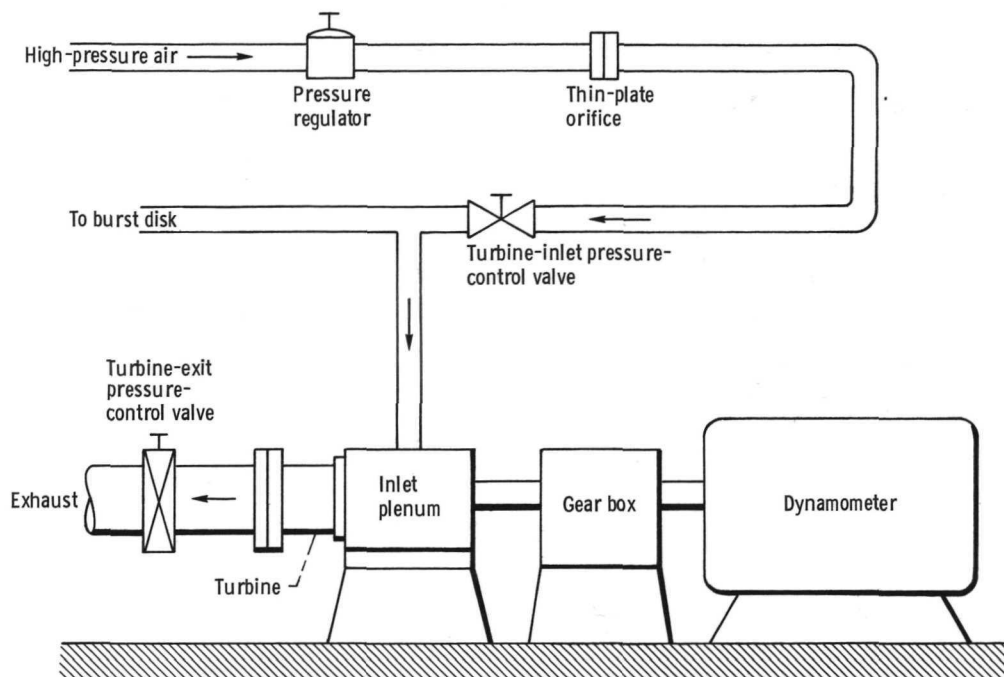
For first-stage operation the second stage was removed and appropriate fairing pieces were inserted to insure smooth flow on the inner and outer walls. A dummy weight was bolted to the shaft to compensate for the weight of the second-stage rotor assembly to keep the turbine critical speed at the same value.

A 300-horsepower cradled dynamometer was used to absorb the turbine power, control speed, and measure torque (fig. 6(a)). The dynamometer was coupled to the turbine shafting through a gear box, which provided relative rotative speeds between dynamometer and turbine of 1.0 to 4.25. Figure 6(b) shows the turbine installed in the test facility.

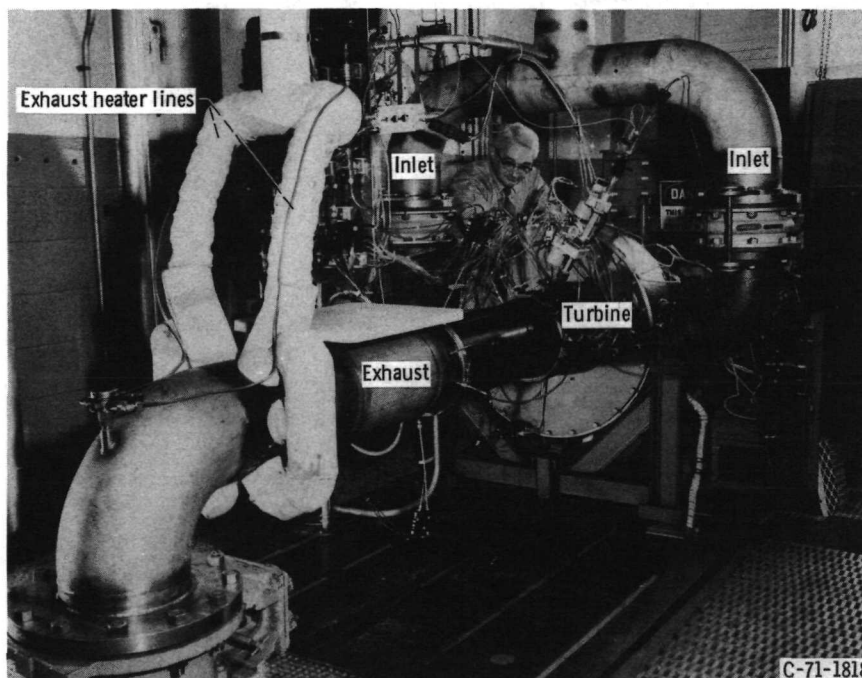
Instrumentation

A torque arm attached to the dynamometer stator transmitted the turbine torque to a commercial strain-gage load cell. This electric signal was sent to the digital voltmeter equipment. The rotational speed was detected by a magnetic pickup and a shaft-mounted gear. The signal was converted to a direct-current voltage and fed into the digital voltmeter.

The instrumentation stations are shown in figure 3. Overall performance for two-stage operation was based on measurements taken at stations 1 and 5. First-stage performance was determined by measurements taken at stations 1 and 3. For first-stage operation the instrumentation at station 3 was identical to that at station 5 during two-stage operation. The instrumentation at the turbine inlet (station 1) consisted of three static-pressure taps equally spaced circumferentially on both the inner and outer walls and three total-temperature rakes each containing three thermocouples. Interstage pressure taps were installed to determine the variation of static pressure through the turbine. There were three tip static-pressure taps equally spaced circumferentially at each of the sta-



(a) Arrangement of piping and test equipment.



(b) Turbine test apparatus.

Figure 6. - Experimental equipment

tions 2, 3, and 4. At station 5, downstream of the rotor exit, the instrumentation consisted of six static-pressure taps equally spaced circumferentially (three each on the inner and outer walls) and a self-aligning probe for flow angle, total temperature, and total pressure measurements. There were also five total-temperature rakes, each containing three thermocouples, at a downstream station 45.7 centimeters (18.0 in.) from the second-stage rotor exit (this station is not seen in fig. 3). These rakes were used primarily as a check on turbine efficiency as calculated from torque measurements. In the calculation of pressure ratio across the turbine, pressure at station 5 was determined from the average of the static pressures at the inner and outer walls.

The values of the pressures at the various stations were measured by transducers. A 200-channel data acquisition system was used to measure and record the electrical signals from the transducers. Figure 7 shows equipment used in converting and transmitting signals received from instrumentation on the turbine. The figure also shows the panels containing the turbine and dynamometer controls.



Figure 7. - Test control room.

Procedure

The turbine was first tested as a two-stage unit. The second stage was then removed and fairing pieces were installed to insure a smooth flow path out of the first stage and provide for the required instrumentation. Data were then obtained for first-stage operation. Performance of the second stage was calculated from the results of these tests.

For the two-stage operation data were obtained at nominal inlet total conditions of 298.9 K (538° R) and 12.4 newtons per square centimeter (18.0 psia). Data were obtained over a range of equivalent-inlet-total- to exit-static pressure ratios from 2.4 to 5.0 and speed range from 0 to 110 percent of equivalent design.

For first-stage operation, data were obtained at nominal inlet total conditions of 295.6 K (532.0° R) and 13.8 newtons per square centimeter (20.0 psia). Data were obtained over a range of equivalent-inlet-total- to exit-static pressure ratios from 1.8 to 4.2 and a speed range from 30 to 110 percent of equivalent design.

The torque calibration was obtained before and after each daily series of runs. An average of these two calibrations was then used in the calculation of turbine torque output. The calibration was obtained with the dynamometer rotating the turbine at a speed of about 2600 rpm. Turbine windage losses were minimized by evacuating the air from the turbine. Most of the effects of turbine rotor windage losses, bearing and seal friction were thus accounted for in the calibration and were not added to the shaft torque when calculating the aerodynamic efficiency of the turbine. By following this calibration procedure, an accuracy of ±0.5 percent of equivalent design torque is estimated in the determination of turbine torque output.

The turbine was rated on the basis of both total and static efficiency. The total pressures were calculated from weight flow, static pressure, total temperature, and flow angle from the following equation:

$$p' = p \left\{ \frac{1}{2} + \frac{1}{2} \left[1 + \frac{2(\gamma - 1)}{\gamma} \frac{R}{g} \left(\frac{w \sqrt{T'}}{pA \cos \alpha} \right)^2 \right]^{1/2} \right\}^{\gamma/(\gamma-1)}$$

In the calculation of turbine-inlet total pressure, the flow angle was assumed to be zero.

RESULTS AND DISCUSSION

The results of this investigation are presented in two sections covering first- and two-stage performance, respectively. All data are shown in terms of equivalent air values. Experimental design-point performance results are given in table IV, along with

the values assumed in the design. This table should aid in the discussion of the results for both first-stage and two-stage performance. The experimental results include overall performance in terms of equivalent mass flow, equivalent specific work, and efficiency. Included are variations of turbine-outlet flow angle, tip static-pressure distribution through the turbine, and rotor-exit radial survey of flow angle at equivalent design speed and pressure ratio.

First-Stage Performance

Overall performance. - The basic data obtained from the turbine tests are shown in figures 8 and 9 with equivalent torque $\epsilon\tau/\delta$ and equivalent mass flow $\epsilon w\sqrt{\theta_{cr}}/\delta$ shown as a function of total- to static-pressure ratio p'_1/p_3 . The performance maps of figure 10 were obtained from crossplots, computed from faired values of figures 8 and 9 as well as similar plots using total to total pressure ratio p'_1/p'_3 . The performance map consists of equivalent specific work $\Delta h/\theta_{cr}$ as a function of the mass-flow - speed parameter $\epsilon w\omega/\delta$ for the various equivalent speeds investigated. Lines of constant pressure ratio and efficiency contours are superimposed. Figure 10(a) shows performance in terms of total conditions. Turbine efficiencies of 0.70 to 0.935 were obtained for the range of pressure ratios and speeds investigated. At equivalent design speed and a design specific work $\Delta h/\theta_{cr}$ of 45.83 joules per gram (19.69 Btu/lb); the total efficiency is slightly greater than 0.93. At equivalent design speed and an equivalent design-inlet to rotor-exit total-pressure ratio of 2.018, a total efficiency of about 0.93 was obtained. This is considerably higher than the design value of 0.870. The design efficiency was used essentially for obtaining rotor-exit conditions and was selected from curves shown in reference 2. These curves were considered to represent reasonable levels of efficiency for actual operation in the turbofan engine. Some factors contributing to the higher efficiency would be small rotor tip clearance, with the clearance being obtained by a recess in the casing instead of reducing rotor-blade tip diameter, as well as the use of some exit whirl compared with zero exit whirl used in the curves of reference 2. Use of some exit whirl results in higher reaction compared with the case with zero exit whirl. Reference 6 presents the experimental results of a 76-centimeter (30-in.) single-stage turbine having comparable solidity, aspect ratio, and speed-work parameter as for the subject turbine. A total efficiency of 0.923, obtained at equivalent design specific work and equivalent design speed, was significantly higher than the 0.885 value assumed in the design. The reference report compared design-point performance of the turbine with that predicted by another procedure (ref. 7), that considered the various losses within the turbine to a greater detail than that considered in reference 2. These results indicated a total efficiency of 0.929 would be obtained for the turbine of reference 6. In view of this

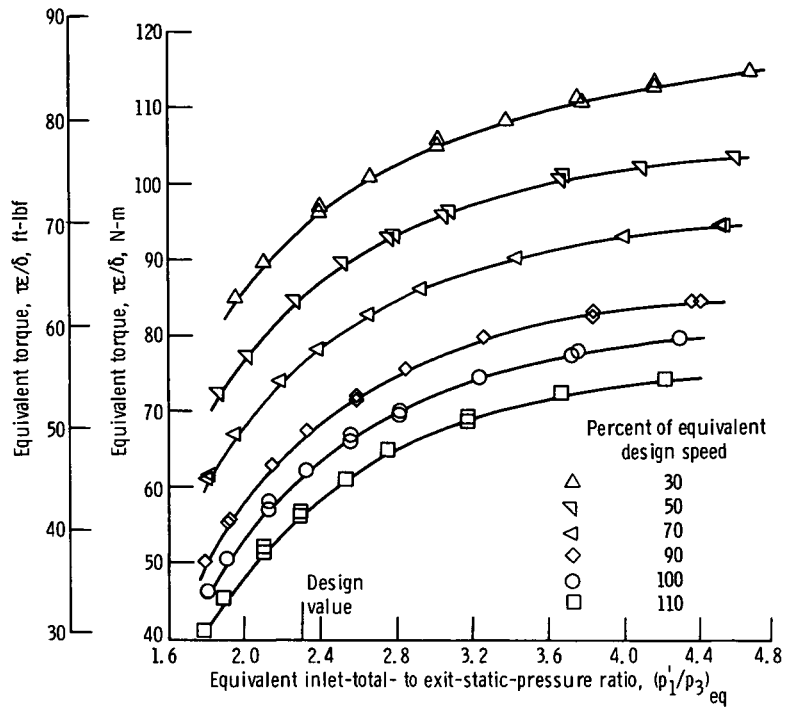


Figure 8. - Variation of torque with pressure ratio and speed for first-stage operation.

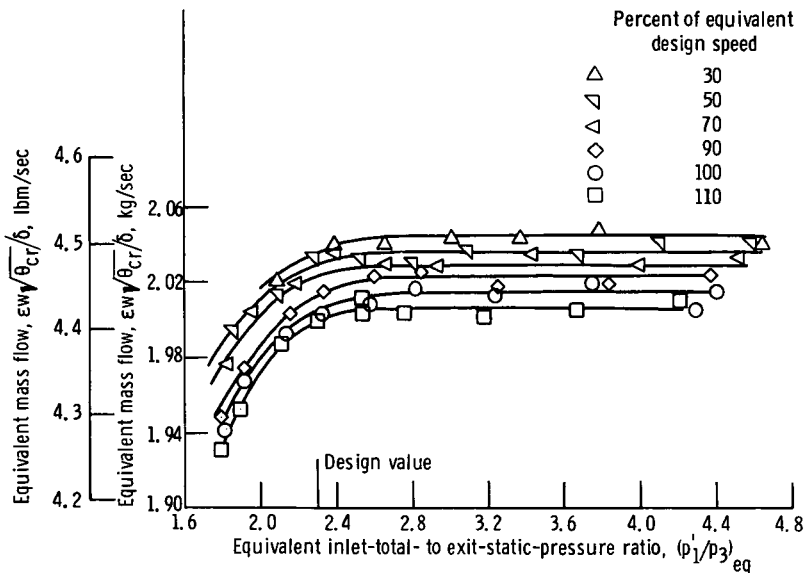


Figure 9. - Variation of mass flow with pressure ratio and speed for first-stage operation.

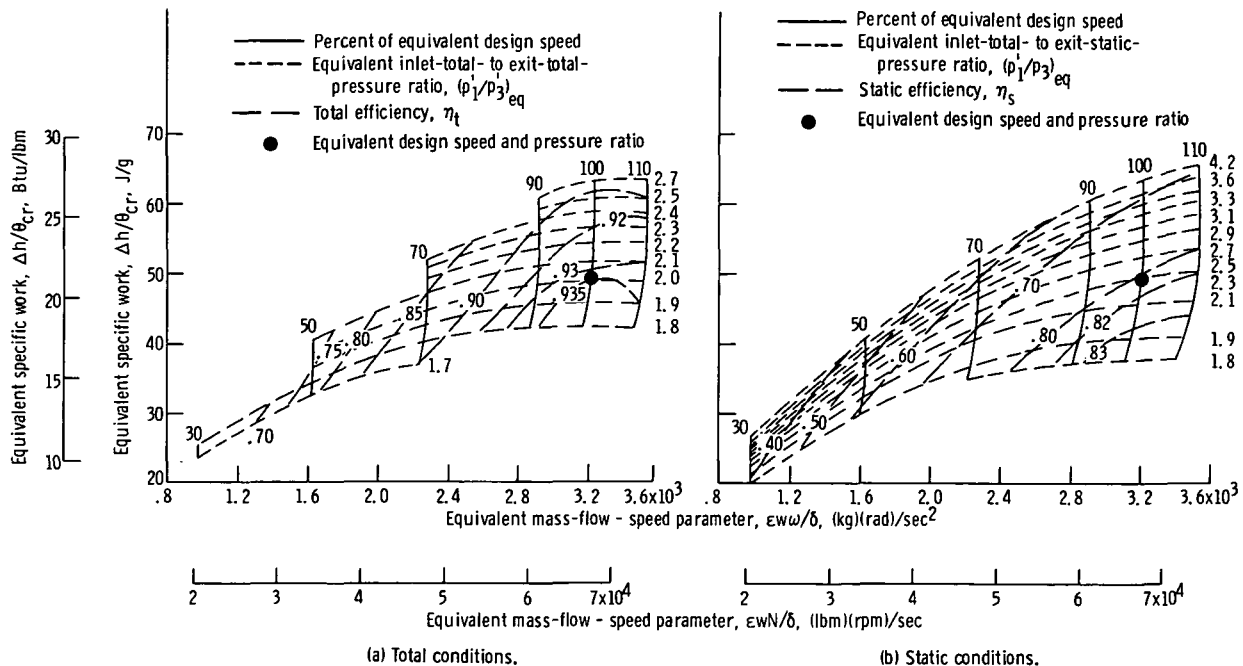


Figure 10. - Overall turbine performance map for first-stage operation.

it appears that the total efficiency value of 0.93 is consistent with that expected for a turbine having similar aerodynamic parameters, as listed in table II.

Figure 10(b) shows the performance of the turbine based on static conditions. At the design equivalent work of 45.834 joules per gram (19.690 Btu/lb) and at equivalent design speed, the static efficiency was slightly over 0.82 which is significantly higher than the 0.747 of the design. The static efficiency was slightly greater than 0.800 at equivalent design pressure ratio (2.298) and at equivalent design speed. Comparison between total and static efficiencies at equivalent design pressure ratio and speed shows that there were 13 points in efficiency in terms of kinetic energy. It should be pointed out that this kinetic energy is available for the second-stage stator.

Mass flow. - Equivalent mass flow is shown in figure 11 as a function of total-to-total pressure ratio. An equivalent mass flow of 2.005 kilograms per second (4.420 lbm/sec) was obtained at equivalent design pressure ratio and speed. This value of mass flow is about 0.8 percent greater than the design value of 1.989 kilograms per second (4.385 lb/sec). The stator-throat area was found to be about 1 percent smaller than design. The reason for the mass flow being slightly greater than design value was primarily due to the rotor-throat area. Since the actual rotor losses were smaller than the design value, the rotor-throat area was therefore larger than required. The larger rotor-throat area resulted in a lower stator-exit static pressure at the stage design pressure ratio and this lower stator-exit static pressure resulted in a greater mass-flow rate.

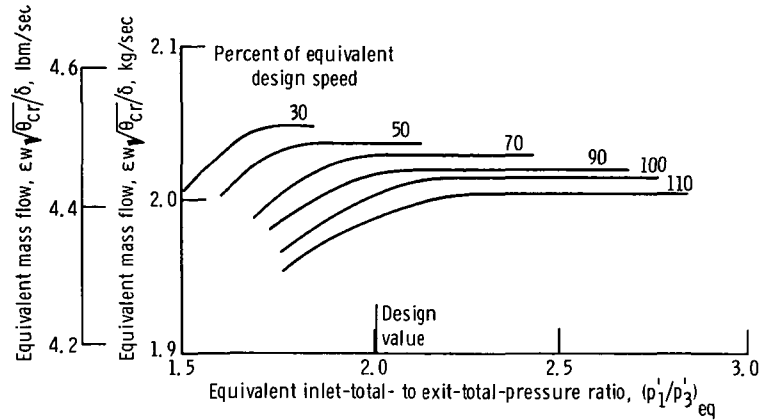


Figure 11. - Variation of mass flow with total-pressure ratio and speed for first-stage operation.

Figure 11 also shows the speed effect on mass flow. Choked flow was obtained at a total pressure ratio of 1.74 at 30 percent of equivalent design speed and at a pressure ratio of about 2.30 at 110 percent of equivalent design speed.

Static-pressure distribution. - Figure 12 shows the tip static-pressure distribution across the first stage. Also shown in the figure is the design static-pressure distribution. The data were obtained at equivalent design speed and pressure ratio. The stator-exit pressure is lower than design as a result of the rotor-throat area being larger than that required for the actual losses through the rotor. This was discussed previously in the mass-flow section. Comparison of pressure levels also shows that the rotor operated with less than design reaction at the tip section.

Rotor exit flow angle. - Figure 13 shows the variation of rotor-exit flow angle as a function of pressure ratio for lines of constant equivalent speed. The flow angles were measured at the mean radius. Negative angles indicate a positive contribution to the specific work. At equivalent pressure ratio and speed, the experimentally obtained rotor-exit flow angle was about -26.5° (compared with the -26.1° for design). Since there was little difference in flow angle, the increased specific work was primarily the result of the overexpansion of the flow in the stator with only a small contribution by the rotor-exit tangential velocity.

Calculations showed that three-fourths of the increase in work was due to the increased rotor-inlet whirl. The rotor-inlet whirl was calculated in the following manner.

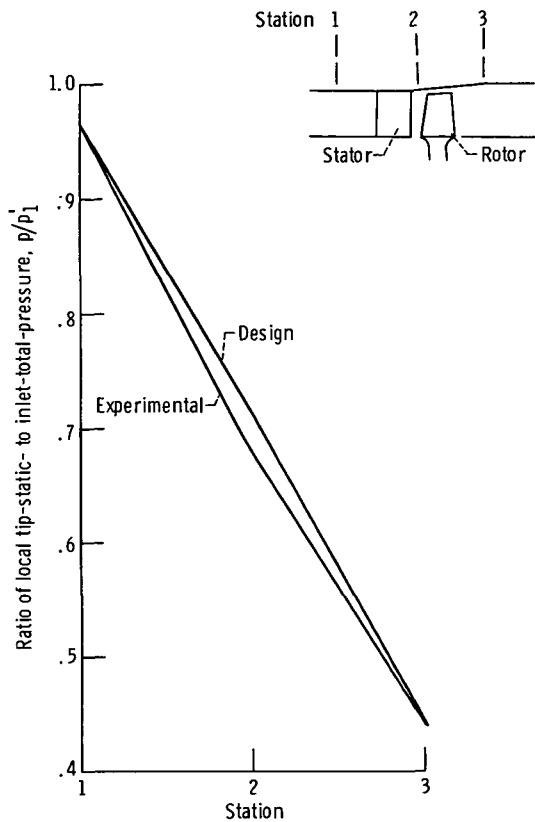


Figure 12. - Variation of tip-static pressure with axial station for first-stage operation at equivalent design speed and design total-to-static-pressure ratio.

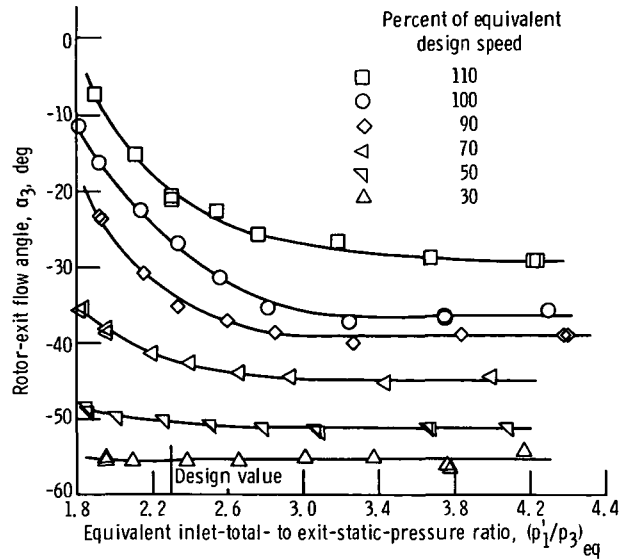


Figure 13. - Variation of rotor-exit flow angle (at the mean radius) with pressure ratio and speed for first-stage operation.

The mass averaged rotor-exit whirl was calculated from rotor-exit static pressure and the result of the rotor-exit radial survey of total temperature, total pressure, and flow angle obtained at equivalent design speed and pressure ratio. The inlet whirl can then be determined from the known blade speed, specific work, and the mass averaged rotor-exit whirl.

Figure 13 also shows that the variation of flow angle with pressure ratio decreases with decreasing speed. The rotor-exit flow angle was essentially constant for the range of pressure ratios investigated at 30 percent of equivalent design speed.

Figure 14 shows the results of a radial angle survey taken at the rotor exit for equivalent design speed and pressure ratio. The figure shows that there was a small amount of overturning over most of the rotor-blade height. As pointed out previously, this small amount of overturning contributed about one-fourth of the increased specific work at equivalent design speed and pressure ratio.

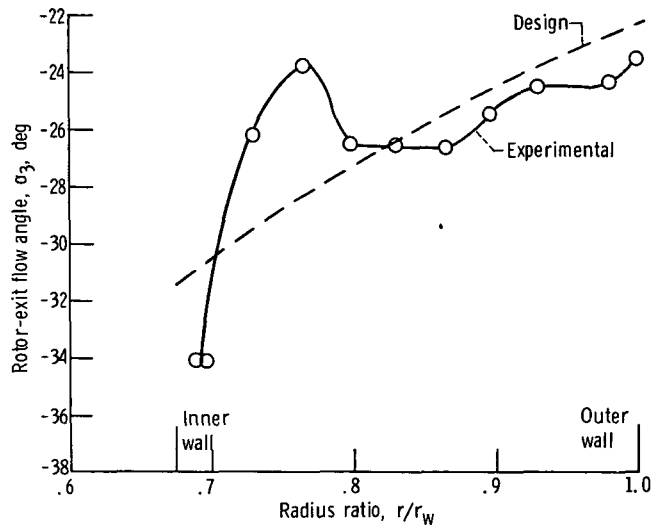


Figure 14. - Variation of rotor-exit flow angle with radius ratio for first-stage operation at equivalent design speed and pressure ratio.

Two-Stage Performance

Overall performance. - Data obtained from the two-stage turbine tests are shown in figures 15 and 16. Equivalent torque $\epsilon\tau/\delta$ and equivalent mass flow $\epsilon w\sqrt{\theta_{cr}}/\delta$ are shown as a function of total to static-pressure ratio p'_1/p_5 . The performance maps of figure 17 were obtained from crossplots, which were computed from faired values of figures 15 and 16 as well as similar plots using total to total pressure ratio p'_1/p'_5 . The performance map consists of equivalent specific work $\Delta h/\theta_{cr}$ as a function of the mass-flow - speed parameter $\epsilon w\omega/\delta$ for the various equivalent speeds investigated. Lines of constant pressure ratio and efficiency contours are superimposed.

Figure 17(a) shows the two-stage performance based on total conditions. The figure shows that a total efficiency value of about 0.93 was obtained at equivalent design speed and pressure ratio. This is significantly higher than the design value of 0.88 assumed in the design. The reason for the difference in efficiency was discussed in the section dealing with the first-stage performance. The figure also shows that the efficiency varied from 0.60 near 30 percent design speed to about 0.93 at 100 percent design speed. The vertical speed lines indicate that the turbine was choked over most of the range of pressure ratios investigated.

Figure 17(b) shows the performance map of the two-stage turbine based on turbine-inlet total- to exit-static conditions. Static efficiency varied from below 0.60 to a peak value slightly higher than 0.85. A static efficiency of 0.82 was obtained at equivalent design speed and pressure ratio. This efficiency value is four points higher than the 0.78 assumed in the design. Comparison of total and static efficiency at design point operation

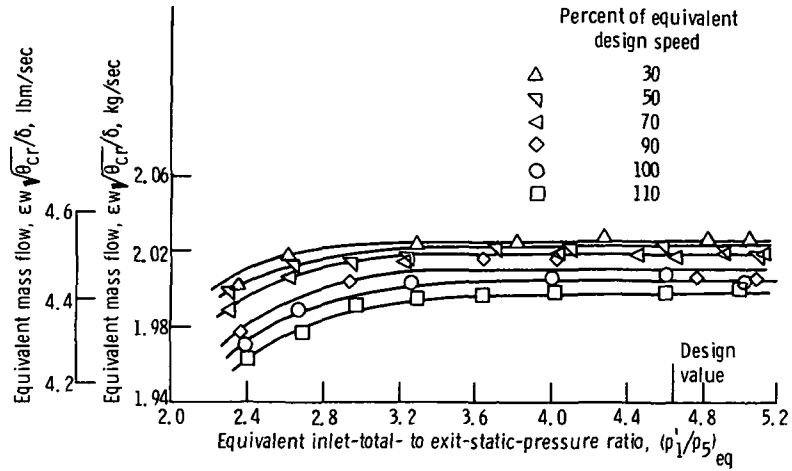


Figure 16. - Variation of mass flow with total- to static-pressure ratio and speed for two-stage operation.

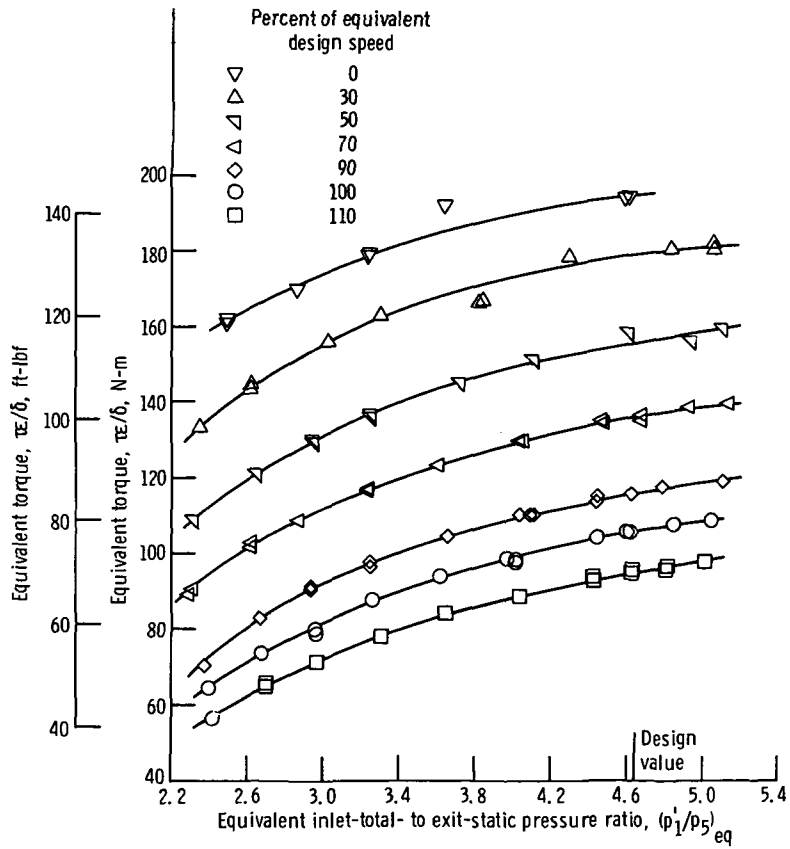
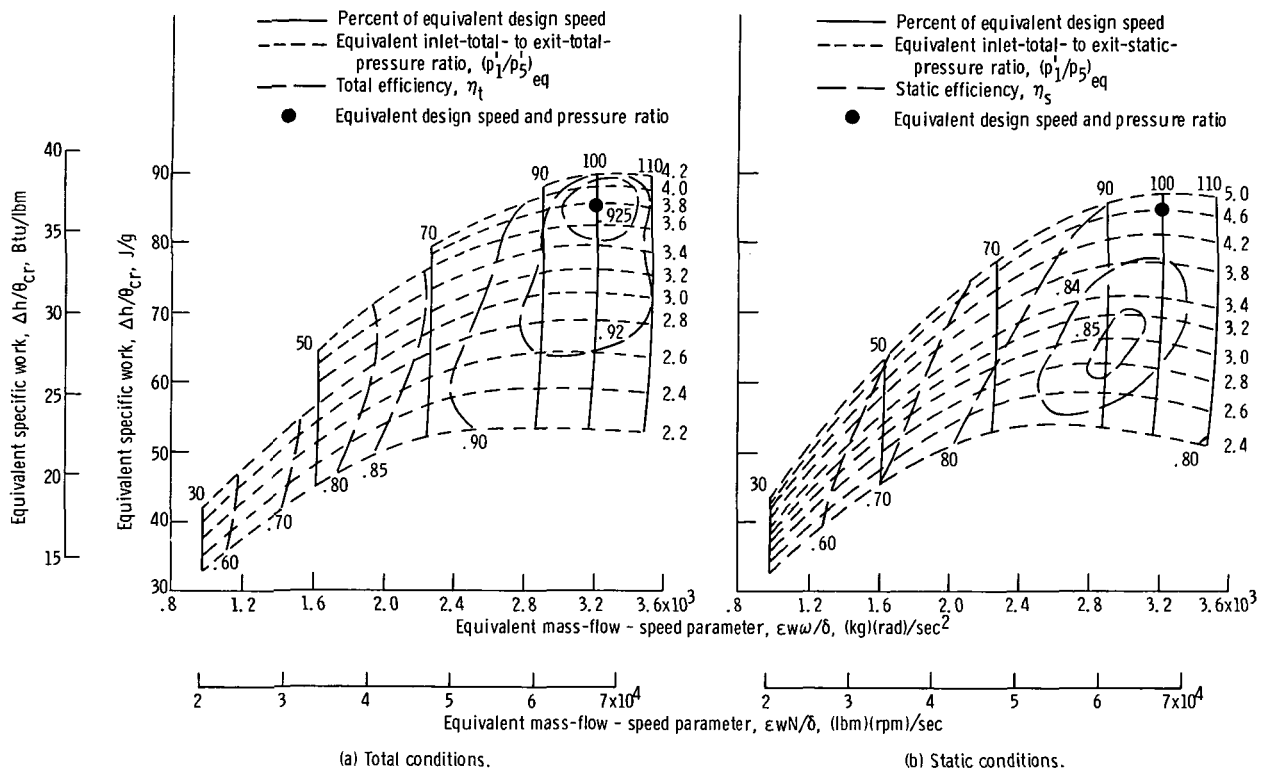


Figure 15. - Variation of torque with pressure ratio and speed for two-stage operation.



shows that there were 11 points in efficiency in terms of kinetic energy.

Although the experimental tests indicated that the turbine was performing significantly better than design, it does not necessarily follow that the same turbine performance would be obtained in the actual engine. Factors such as nonuniform inlet conditions of pressure and temperature, increased leakage, and increased tip clearance would reduce the performance to a value somewhat closer to the design value. The inlet conditions to the turbine, for the reported investigation, were optimum for minimum losses. There was no leakage around the first-stage stator, and the second-stage stator had a labyrinth seal to minimize leakage. In addition, the recessed casing with minimum tip clearance also contributed to minimizing the losses.

Performance of the second stage under two-stage operation was estimated by the use of first- and two-stage performance and the tip static-pressure variation through the turbine. The results indicated that, at equivalent design speed and pressure ratio, a total efficiency of 0.91 and static efficiency of 0.69 was obtained for the second stage. Design values were 0.871 and 0.669, respectively. The total efficiency was, therefore, four points higher than design. At design point operation, the work split was 58 percent for the first stage and 42 percent for the second stage. This work split agrees favorably with the 57 to 43 percent work split selected in the design.

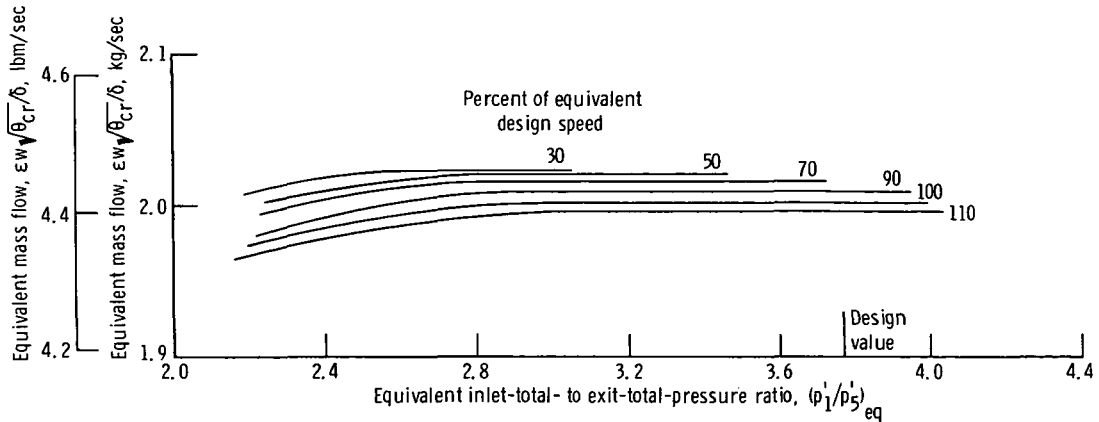


Figure 18. - Variation of mass flow with total-pressure ratio and speed for two-stage operation.

Mass flow. - Figure 18 shows the variation of mass flow as a function of turbine inlet total to exit total pressure ratio for lines of constant equivalent speed. The turbine chokes at a pressure ratio of about 2.6 at 30 percent design speed and at a pressure ratio of about 3.1 at 110 percent of design speed. The equivalent mass flow was 2.004 kilograms per second (4.418 lbm/sec) at equivalent design speed and pressure ratio (3.765). This value of mass flow is about 0.8 percent higher than the design value of 1.989 kilograms per second (4.385 lbm/sec). Measurements of stator throat areas indicated that the first-stage-stator throat area was about 1 percent smaller than design and that the second-stage-stator throat area was about 3.3 percent larger than design value.

Static-pressure distribution. - Figure 19 shows the tip static-pressure variation through the turbine for two-stage operation at equivalent design speed and pressure ratio. The figure shows that the pressure level was lower than design through the turbine. The lower pressure level was the result of the rotor throat areas being oversized because of the higher losses assumed in the design.

Rotor-exit flow angle. - Figure 20 shows the radial variation in flow angle with radius ratio for two-stage operation at equivalent design speed and pressure ratio. Underturning was obtained over most of the rotor blade height. Increased whirl in the stators and first-stage rotor accounted for the increased specific work obtained at equivalent design speed and pressure ratio.

Figure 21 shows the variation of rotor-exit flow angle with pressure ratio for lines of constant speed. Specific work increases as the flow angle decreases. This figure was included in the report for use in off-design prediction and simulation.

Experimental design point performance results are given in table IV, along with the values assumed in the design, in a summation of the results for both first-stage and two-stage performance.

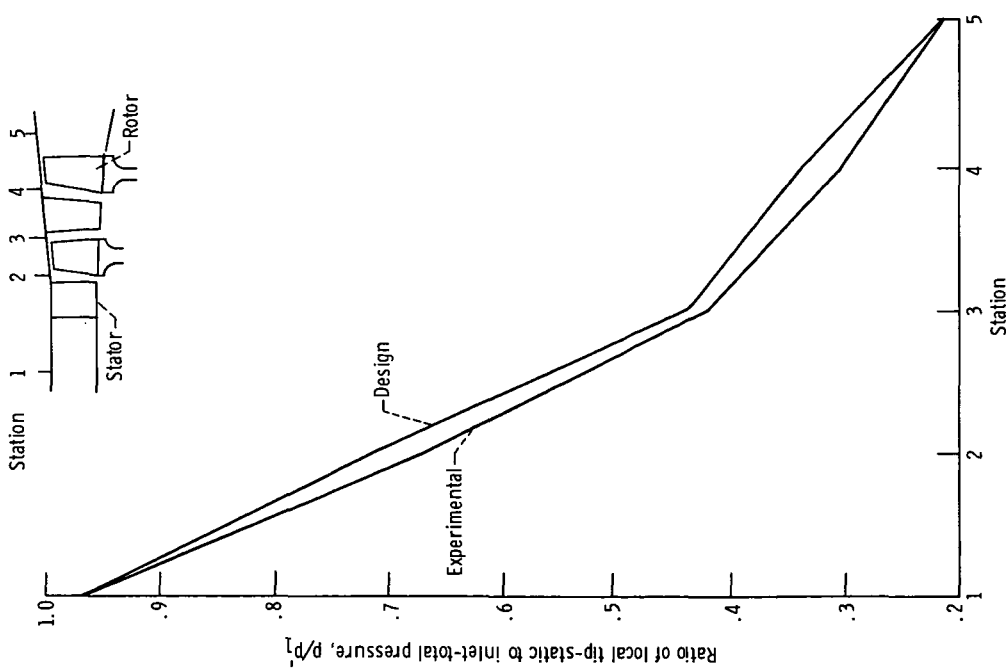


Figure 19. - Variation of tip-static pressure through turbine at equivalent design speed and design total-to-static-pressure ratio.

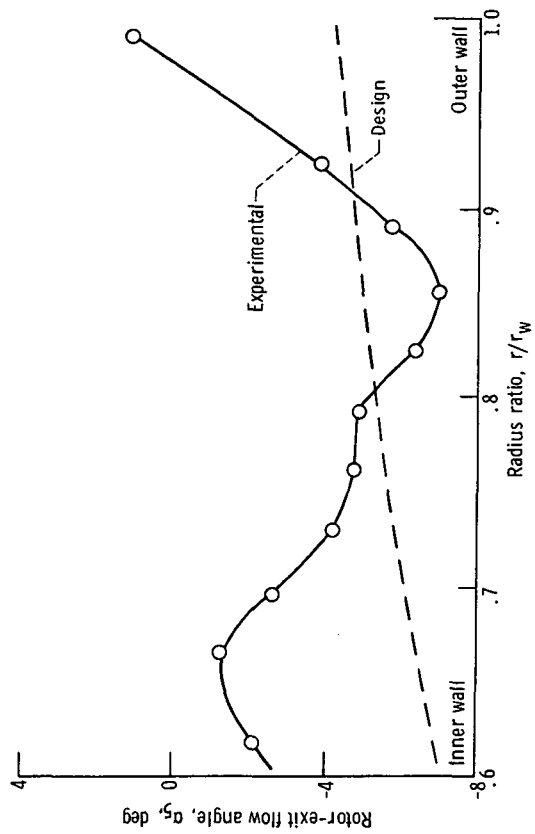


Figure 20. - Variation of rotor-exit flow angle with radius ratio for two-stage operation at equivalent design speed and pressure ratio.

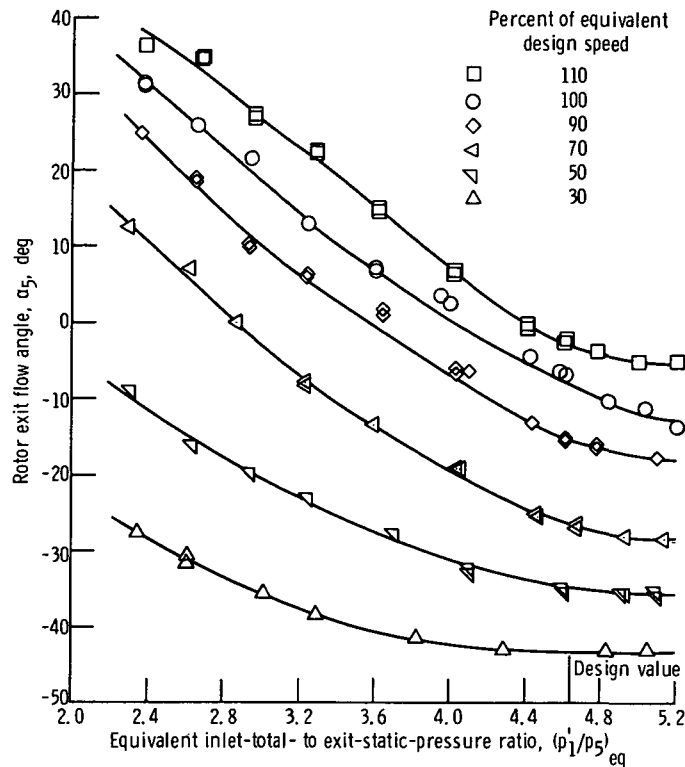


Figure 21. - Variation of rotor-exit flow angle (at the mean diameter) with pressure ratio and speed for two-stage operation.

SUMMARY OF RESULTS

An experimental investigation of a two-stage axial-flow turbine with a mean diameter of 20.32 centimeters (8.00 in.) was made to determine the performance level over a range of speeds and pressure ratios. The turbine was designed to drive the fan and compressor of a turbofan engine suitable for light aircraft application. Performance characteristics were obtained for both first-stage and two-stage operation. The results of this investigation are summarized in the following sections.

First-Stage Operation

(1) Total and static efficiencies of 0.93 and 0.80 were obtained at equivalent design speed and pressure ratio. These values are significantly higher than the total and static efficiency values of 0.870 and 0.747 assumed in the design. The difference between the experimental and design values was attributed to the method used in establishing the design efficiency level.

(2) The experimental mass flow at equivalent design speed and pressure ratio was 2.005 kilograms per second (4.420 lbm/sec). This value of mass flow represents about an 0.8 percent increase over the design value even though the stator throat area was found to be about 1 percent lower than design value.

(3) Lower static pressure was obtained through the stator and was attributed to the excessive rotor throat area due to the assumed design losses being greater than the actual losses.

Two-Stage Operation

(1) Total and static efficiencies of 0.93 and 0.82, respectively, were obtained at equivalent design speed and pressure ratio. These efficiency values were significantly higher than the 0.880 and 0.780 values, respectively, assumed in the design.

(2) The equivalent mass flow was 2.004 kilograms per second (4.418 lbm/sec) at equivalent design speed and pressure ratio. This mass flow value was about 0.8 percent greater than the design value.

(3) The tip static-pressure variation through the turbine indicated a pressure level lower than design in all blade rows with the exception of the last stage rotor. The lower pressure level was the result of the excess rotor throat area due to the assumed losses being greater than the actual losses.

(4) The experimentally obtained work split at equivalent design speed and pressure ratio was 58 percent for the first stage and 42 percent for the second stage. This work split agrees favorably with the 57- to 43-percent work split selected in the design. At design point operation first- and second-stage total efficiencies were 0.93 and 0.91 or six and four points higher than design, respectively.

CONCLUDING REMARKS

Although the experimental turbine performance was considerably better than design, the high efficiency values would not necessarily be expected in actual engine operation. Losses due to nonuniform turbine inlet conditions, increased interstage leakage, and increased tip clearance could result in efficiencies closer to the design values than those obtained in this cold-air investigation.

Lewis Research Center,
National Aeronautics and Space Administration,
Cleveland, Ohio, June 28, 1972,
112-27.

REFERENCES

1. Cummings, Robert L. ; and Gold, Harold: Concepts for Cost Reduction on Turbine Engines for General Aviation. NASA TM X-52951, 1971.
2. Stewart, Warner L. : A Study of Axial-Flow Turbine Efficiency Characteristics in Terms of Velocity Diagram Parameters. Paper 61-WA-37, ASME, Nov. 1961.
3. Miser, James W. ; Stewart, Warner L. ; and Whitney, Warren J. : Analysis of Turbo-machine Viscous Losses Affected by Changes in Blade Geometry. NACA RM E56F21, 1956.
4. Katsanis, Theodore; and Dellner, Lois T. : A Quasi-Three-Dimensional Method for Calculating Blade Surface Velocities for an Axial Flow Turbine Blade. NASA TM X-1394, 1967.
5. Miser, James W. ; Stewart, Warner L. ; and Wong, Robert Y. : Effect of a Reduction in Stator Solidity on Performance of a Transonic Turbine. NACA RM E55L09a, 1956.
6. Whitney, Warren J. ; Szanca, Edward M. ; Bider, Bernard; and Monroe, Daniel E. : Cold-Air Investigation of a Turbine for High-Temperature-Engine Application. III - Overall Stage Performance. NASA TN D-4389, 1968.
7. Ainley, D. G. ; and Mathieson, G. C. R. : A Method of Performance Estimation for Axial-Flow Turbines. Rep. R & M-2974, Aeronautical Research Council, Great Britain, 1957.

TABLE I. - TURBINE DESIGN OPERATING VALUES

	First-stage	Two-stage
For operation with fuel mixture (hydrogen/carbon = 0.167):		
Inlet total temperature, T_1' , K; °R	977.78; 1760	977.78; 1760
Inlet total pressure, p_1' , N/cm ² abs; psia	28.544; 41.40	28.544; 41.40
Mass flow, w, kg/sec; lb/sec	2.994; 6.60	2.994; 6.60
Turbine rotative speed, N, rpm	28 000	28 000
Rotor blade speed (mean section); m/sec; ft/sec	297.91; 977.38	297.91; 977.38
Total- to static-pressure ratio, p_1'/p_3 or 5	2.238	4.312
Total- to total-pressure ratio, p_1'/p_3 or 5	1.975	3.551
Blade-jet speed ratio, ν	0.466	0.360
Work-speed parameter, λ	0.582	0.331
Total- to static-efficiency, η_s	0.747	0.780
Total- to total-efficiency, η_t	0.870	0.880
Specific work, Δh , J/g; Btu/lb	152.77; 65.63	268.02; 115.14
Air equivalent:		
Mass flow, $\epsilon w \sqrt{\theta_{cr}}/\delta$, kg/sec; lb/sec	1.989; 4.385	1.989; 4.385
Specific work, $\Delta h/\theta_{cr}$, J/g; Btu/lb	45.834; 19.690	80.407; 34.542
Torque, $\tau\epsilon/\delta$, newton-meter; ft-lb	56.727; 41.840	99.521; 73.403
Rotative speed, $N/\sqrt{\theta_{cr}}$, rpm	15 336	15 336
Rotor blade speed (mean section), m/sec; ft/sec	163.17; 535.33	163.17; 535.33
Total- to static-pressure ratio (p_1'/p_3 or 5) eq	2.298	4.640
Total- to total-pressure ratio (p_1'/p_3 or 5) eq	2.018	3.765
Blade-jet speed ratio, ν	0.466	0.360
Work-speed parameter, λ	0.582	0.331

TABLE II. - TURBINE AERODYNAMIC PARAMETERS

Turbine stage	Blade row	Section	Blade-surface diffusion parameter ^a			Blade turning, deg	Blade chord,		Solidity	Reaction ^a	Aspect ratio ^b	Number of blades	Tip clearance,	
			Suction surface, D_s	Pressure surface, D_p	Total, D_{tot}		cm	in.					cm	in.
First	Stator	Tip	0.159	0.317	0.476	68.7	2.946	1.160	1.39	0.643	1.29	35		
		Mean	.131	.309	.440	65.0	2.616	1.030	1.43	.684				
		Hub	.089	.277	.366	61.5	2.400	.945	1.35	.729				
	Rotor	Tip	0.211	0.504	0.715	63.9	2.654	1.045	1.50	0.619	1.39	42	0.030	0.012
		Mean	.151	.338	.489	91.2	2.606	1.026	1.71	.529				
		Hub	.211	.458	.669	111.0	2.758	1.086	2.18	.301				
Second	Stator	Tip	0.277	0.356	0.633	72.0	2.517	0.991	1.42	0.387	1.95	43		
		Mean	.250	.428	.678	81.3	2.182	.859	1.47	.444				
		Hub	.182	.456	.638	92.9	1.864	.734	1.56	.543				
	Rotor	Tip	0.176	0.157	0.333	38.8	2.372	0.934	1.34	0.463	1.98	44	0.038	0.015
		Mean	.231	.128	.359	62.8	2.408	.948	1.66	.402				
		Hub	.251	.247	.498	85.1	2.438	.960	2.16	.114				

^aSee the section SYMBOLS for definition.

^bBased on average blade height and mean blade chord.

TABLE III. - BLADE SECTION COORDINATES

(a) Stator

[Trailing-edge radius, 0.025.]

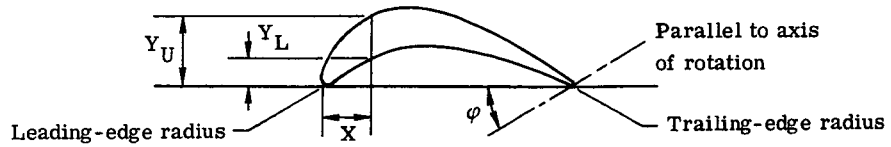


X	First stage						Second stage					
	Hub		Mean		Tip		Hub		Mean		Tip	
	Radius, cm											
	8.479	10.160	11.844	8.186	10.160	12.128						
	angle, deg											
	43.65	43.03	39.97	30.72	28.72	27.12						
	Leading-edge radius, cm											
	0.127						0.097					
	Y_U	Y_L	Y_U	Y_L	Y_U	Y_L	Y_U	Y_L	Y_U	Y_L	Y_U	Y_L
0	0.127	0.127	0.127	0.127	0.127	0.127	0.097	0.097	0.097	0.097	0.097	0.097
.127	.445	.000	.424	.000	.427	.000	.330	.005	.300	.005	.274	.005
.254	.559	.056	.538	.043	.549	.036	.457	.119	.417	.097	.378	.069
.381	.615	.119	.599	.094	.625	.081	.526	.206	.493	.165	.452	.127
.508	.643	.173	.632	.135	.671	.124	.556	.257	.538	.213	.503	.168
.635	.653	.211	.650	.170	.696	.160	.561	.282	.561	.244	.533	.201
.762	.648	.241	.653	.198	.706	.191	.549	.292	.569	.264	.549	.218
.889	.632	.259	.648	.216	.706	.218	.521	.284	.561	.269	.549	.229
1.016	.610	.267	.632	.224	.696	.236	.480	.267	.538	.267	.538	.231
1.143	.579	.267	.612	.229	.681	.249	.432	.241	.513	.254	.521	.224
1.270	.544	.257	.584	.226	.658	.257	.376	.206	.475	.239	.498	.213
1.397	.503	.241	.549	.221	.630	.262	.312	.165	.429	.216	.470	.198
1.524	.457	.221	.511	.211	.602	.257	.246	.119	.378	.185	.437	.180
1.651	.406	.196	.467	.196	.564	.249	.178	.074	.320	.152	.399	.165
1.778	.351	.165	.422	.175	.523	.234	.097	.023	.259	.117	.358	.147
1.864	-----	-----	-----	-----	-----	-----	.025	.025	-----	-----	-----	-----
1.905	.295	.132	.378	.150	.483	.218	-----	-----	.193	.079	.315	.127
2.032	.234	.097	.320	.122	.439	.196	-----	-----	.124	.038	.267	.104
2.159	.173	.061	.264	.094	.394	.170	-----	-----	-----	-----	.216	.079
2.182	-----	-----	-----	-----	-----	-----	-----	-----	.025	.025	-----	-----
2.286	.104	.025	.203	.069	.343	.142	-----	-----	-----	-----	.155	.051
2.400	.025	.025	-----	-----	-----	-----	-----	-----	-----	-----	-----	-----
2.413	-----	-----	.145	.038	.287	.117	-----	-----	-----	-----	.094	.020
2.517	-----	-----	-----	-----	-----	-----	-----	-----	-----	-----	.025	.025
2.540	-----	-----	.084	.010	.231	.089	-----	-----	-----	-----	-----	-----
2.616	-----	-----	.025	.025	-----	-----	-----	-----	-----	-----	-----	-----
2.667	-----	-----	-----	-----	.178	.061	-----	-----	-----	-----	-----	-----
2.794	-----	-----	-----	-----	.117	.030	-----	-----	-----	-----	-----	-----
2.921	-----	-----	-----	-----	.058	.000	-----	-----	-----	-----	-----	-----
2.946	-----	-----	-----	-----	.025	.025	-----	-----	-----	-----	-----	-----

TABLE III. - Concluded. BLADE SECTION COORDINATES

(b) Rotor

[Trailing-edge radius, 0.025.]



X	First stage						Second stage					
	Hub		Mean		Tip		Hub		Mean		Tip	
	Radius, cm											
	8.471	10.160	11.839	7.915	10.160	12.413						
	angle, deg											
	17.07	31.05	42.00	5.25	21.75	37.67						
	Leading-edge radius, cm											
	0.097	0.081	0.064	0.097	0.081	0.064						
	Y _U	Y _L	Y _U	Y _L	Y _U	Y _L	Y _U	Y _L	Y _U	Y _L	Y _U	Y _L
0	0.097	0.097	0.081	0.081	0.064	0.064	0.097	0.097	0.081	0.081	0.064	0.064
.127	.396	.005	.366	.018	.312	.030	.259	.005	.226	.015	.178	.018
.254	.607	.142	.531	.112	.437	.124	.368	.084	.315	.074	.241	.053
.381	.762	.279	.632	.196	.511	.196	.462	.157	.386	.124	.290	.081
.508	.874	.389	.704	.257	.559	.244	.541	.218	.442	.168	.323	.102
.635	.955	.472	.744	.310	.587	.282	.599	.269	.483	.203	.345	.117
.762	1.011	.533	.767	.343	.599	.305	.640	.312	.503	.229	.361	.130
.889	1.039	.574	.772	.368	.594	.318	.665	.345	.518	.249	.366	.137
1.016	1.049	.599	.765	.381	.584	.320	.676	.366	.521	.259	.366	.137
1.143	1.044	.615	.742	.389	.564	.315	.676	.376	.513	.264	.356	.132
1.270	1.021	.620	.711	.381	.538	.307	.660	.378	.498	.259	.340	.127
1.397	.988	.610	.671	.373	.508	.292	.632	.371	.472	.249	.320	.119
1.524	.940	.592	.627	.358	.470	.274	.594	.356	.439	.234	.295	.107
1.651	.884	.564	.572	.335	.432	.251	.549	.330	.396	.208	.269	.097
1.778	.818	.533	.513	.305	.391	.224	.493	.295	.351	.178	.234	.081
1.905	.744	.493	.450	.267	.348	.193	.427	.249	.300	.142	.198	.066
2.032	.655	.437	.386	.226	.302	.163	.353	.196	.241	.107	.160	.048
2.159	.561	.373	.320	.180	.254	.130	.267	.137	.178	.069	.117	.030
2.286	.462	.302	.251	.127	.206	.097	.173	.071	.112	.030	.076	.010
2.372	-----	-----	-----	-----	-----	-----	-----	-----	-----	-----	.025	.025
2.408	-----	-----	-----	-----	-----	-----	-----	-----	.025	.025	-----	-----
2.413	.358	.224	.170	.017	.152	.056	-----	-----	-----	-----	-----	-----
2.438	-----	-----	-----	-----	-----	-----	.025	.025	-----	-----	-----	-----
2.540	.246	.137	.086	.013	.097	.025	-----	-----	-----	-----	-----	-----
2.606	-----	-----	.025	.025	-----	-----	-----	-----	-----	-----	-----	-----
2.654	-----	-----	-----	-----	.025	.025	-----	-----	-----	-----	-----	-----
2.667	.127	.046	-----	-----	-----	-----	-----	-----	-----	-----	-----	-----
2.758	.025	.025	-----	-----	-----	-----	-----	-----	-----	-----	-----	-----

TABLE IV. - COMPARISON OF EXPERIMENTAL WITH DESIGN VALUES^a

Stage	Type of value	Efficiency		Equivalent specific work, $\Delta h/\theta_{cr}$		Equivalent mass flow, $\epsilon w \sqrt{\theta_{cr}}/\delta$		Equivalent torque	
		Total, η_t	Static, η_s	J/g	Btu/lb	kg/sec	lb/sec	N-M	ft-lb
		First	Design	0.870	0.747	45.83	19.69	1.989	4.385
	Experimental	.93	.80	49.28	21.17	2.005	4.420	61.50	45.36
Second ^a	Design	0.871	0.669	41.00	17.61	3.680	8.114	86.13	63.52
	Experimental	.91	.69	41.39	17.78	3.764	8.299	88.82	65.51
Two	Design	0.88	0.78	80.41	34.54	1.989	4.385	99.27	73.22
	Experimental	.93	.82	84.90	36.47	2.004	4.418	106.00	78.18

^aBased on conditions at inlet of second stage.

OFFICIAL BUSINESS
PENALTY FOR PRIVATE USE \$300

FIRST CLASS MAIL

POSTAGE AND FEES PAID
NATIONAL AERONAUTICS AND
SPACE ADMINISTRATION



NASA 451

POSTMASTER: If Undeliverable (Section 158
Postal Manual) Do Not Return

"The aeronautical and space activities of the United States shall be conducted so as to contribute . . . to the expansion of human knowledge of phenomena in the atmosphere and space. The Administration shall provide for the widest practicable and appropriate dissemination of information concerning its activities and the results thereof."

— NATIONAL AERONAUTICS AND SPACE ACT OF 1958

NASA SCIENTIFIC AND TECHNICAL PUBLICATIONS

TECHNICAL REPORTS: Scientific and technical information considered important, complete, and a lasting contribution to existing knowledge.

TECHNICAL NOTES: Information less broad in scope but nevertheless of importance as a contribution to existing knowledge.

TECHNICAL MEMORANDUMS: Information receiving limited distribution because of preliminary data, security classification, or other reasons.

CONTRACTOR REPORTS: Scientific and technical information generated under a NASA contract or grant and considered an important contribution to existing knowledge.

TECHNICAL TRANSLATIONS: Information published in a foreign language considered to merit NASA distribution in English.

SPECIAL PUBLICATIONS: Information derived from or of value to NASA activities. Publications include conference proceedings, monographs, data compilations, handbooks, sourcebooks, and special bibliographies.

TECHNOLOGY UTILIZATION PUBLICATIONS: Information on technology used by NASA that may be of particular interest in commercial and other non-aerospace applications. Publications include Tech Briefs, Technology Utilization Reports and Technology Surveys.

Details on the availability of these publications may be obtained from:

SCIENTIFIC AND TECHNICAL INFORMATION OFFICE

NATIONAL AERONAUTICS AND SPACE ADMINISTRATION

Washington, D.C. 20546